ISSN 0022-4766, Journal of Structural Chemistry, 2020, Vol. 61, No. 1, pp. 66-72. © Pleiades Publishing, Ltd., 2020.
Text © The Author(s), 2020, published in Zhurnal Strukturnoi Khimii, 2020, Vol. 61, No. 1, pp. 71-77.

SYNTHESIS AND MOLECULAR STRUCTURE OF THE ZINC(II) COMPLEX BEARING AN N, S DONOR LIGAND

J. Haribabu[1], S. Priyarega[2], N. S. P. Bhuvanesh[3], and R. Karvembu[1]*

The reaction between zinc(II) acetate dihydrate and ((1H-indol-3-yl)methylene)-N-methylhydrazinecarbothioamide (L) in methanol results in the formation of Zn(II) complex $[Zn(C_{11}H_{11}N_4S)_2]$ (**1**). The complex is characterized by CHNS and various spectroscopic analyses. The structure of the complex is determined by the single crystal X-ray diffraction technique. XRD reveals that the Zn(II) complex crystallizes in the triclinic system with the *P*-1 space group and has a distorted tetrahedral geometry. Two ligand molecules are coordinated to the Zn(II) ion in the bidentate monobasic (NS^-) fashion.

DOI: 10.1134/S0022476620010072

Keywords: zinc(II) complex, thiosemicarbazone, molecular structure, distorted tetrahedral geometry.

INTRODUCTION

In humans, Zn is considered as the second most essential and abundant transition metal next to iron [1]. It has been a component of over 3000 Zn-associated transcriptions, including DNA-binding proteins with Zn fingers, and more than 300 enzymes, including Cu/Zn superoxide dismutase (CuZnSOD) and several proteins involved in DNA repair [2-4]. In many cellular processes such as cell proliferation, reproduction, immune function and defence against free radicals, zinc has a vital role, which makes it a chief metal [5, 6]. Zn fingers or metallo-regulatory proteins capable of recognizing DNA or nucleotides are the proof that Zn has the capability of establishing non-direct covalent interactions with DNA. Zn is also the only metal ion able to bring about the rewinding of DNA. The extensive use of Zn in the form of "Baby Zinc" in the treatment of deadly diarrhoea has saved the lives of many children in Asian and African countries [7-9].

Furthermore, many Zn complexes have been reported for their biological activities such as anticonvulsant, antidiabetic [10], anti-inflammatory [11], antimicrobial [12-17], antioxidant [18, 19], anti-proliferative/antitumor [11, 12, 20-22], anti-Alzheimer [23], and so on. Zn is an efficient Lewis acid, making it a useful catalytic agent in hydroxylation and other enzymatic reactions. The metal also has a flexible coordination geometry, which allows proteins to use it to rapidly shift conformations to perform biological reactions. Two examples of Zn-containing enzymes are carbonic anhydrase and carboxypeptidase, which are vital to the processes of carbon dioxide (CO_2) regulation and digestion of proteins, respectively [24, 25].

Thiosemicarbazone ligands are a broad class of derivatives of Schiff bases which, over the years, have established their importance in the pharmaceutical arena by exhibiting biological activities against tuberculosis, tumour, fungi and

[1]Department of Chemistry, National Institute of Technology, Tiruchirappalli, India; *kar@nitt.edu. [2]Department of Chemistry, Saranathan College of Engineering, Tiruchirappalli, India. [3]Department of Chemistry, Texas A & M University, College Station, Texas USA. Original article submitted April 22, 2019; revised June 19, 2019; accepted June 20, 2019.

bacteria, inflammations, and a range of viruses [26-33]. Thiosemicarbazones are known to exhibit versatile coordination modes with transition metal ions and coordinate either as a neutral ligand or a deprotonated anion (bidentate N, S donor ligand) forming chelate rings [34]. These metal complexes have their applications spread out from biological to materials sciences fields [35]. Of late, Schiff base zinc complexes have fascinated substantial curiosity due to their various coordination modes and special properties.

EXPERIMENTAL

Materials and methods. Zinc(II) acetate dihydrate, 4-methyl thiosemicarbazide and indole-3-carbaldehyde were purchased from Alfa Aesar. The CHNS analysis was performed using a Vario EL-III CNHS analyzer. Melting point of the compound was determined using a Lab India instrument and is uncorrected. The UV-Visible spectrum was recorded using a Shimadzu-2600 spectrophotometer in a DMF solution. The FT-IR spectrum of the complex was obtained in the range 400-4000 cm^{-1} (KBr pellet) using a Nicolet-iS5 spectrophotometer.

Synthesis of $[Zn(C_{11}H_{11}N_4S)_2]$ complex (1). Firstly, the indole-based thiosemicarbazone ligand ((1H-indol-3-yl)methylene)-N-methylhydrazinecarbothioamide (L) was synthesized from indole-3-carbaldehyde and 4-methyl-3-thiosemicarbazide following the reported procedure [36-38]. To a hot methanolic solution of Zn(II) acetate dihydrate (219 mg, 1 mmol), the solution of the synthesized indole thiosemicarbazone ligand (465 mg, 2 mmol) in methanol was added. The mixture was stirred vigorously and refluxed for 6 h, which was then cooled and the precipitated zinc complex was collected by filtration and dried at room temperature. Recrystallization from a chloroform-dimethylformamide (3:1) mixture afforded yellowish-white crystals suitable for the single crystal X-ray diffraction analysis. Yield: 88%. Colourless solid. M.p.: 218 °C. Anal. calc. for $C_{22}H_{22}N_8S_2Zn$ (%): C 50.05, H 4.20, N 21.22, S 12.15. Found (%): C 50.11, H 4.14, N 21.09, S 12.29. UV-Vis (DMF): λ_{max} (nm) 260, 322, 395. FT-IR (KBr): ν (cm^{-1}) 3435, 3323 (N–H), 1509 (C=N), 721 (C–S).

Crystal structure analysis. A Leica MZ 75 microscope was employed to identify a suitable colourless block with very well defined faces with dimensions 0.276×0.222×0.126 mm from a representative sample of crystals of the same habit. Single crystal X-ray diffraction data of the Zn(II) complex (**1**) were collected using a BRUKER Venture X-ray (kappa geometry) diffractometer at 110 K with Cu–Iμs X-ray tube (K_α = 1.5418 Å with a potential of 50 kV and a current of 1.0 mA). The goniometer was controlled using the APEX3 software suite. Integrated intensity information for each reflection was obtained by reduction of the data frames with program APEX3 [39]. TWINABS was used to correct the data for absorption effects [40]. A solution was obtained readily (Z =6; Z' =3) using XT/XS in APEX3 [39, 41-43]. The H atoms were placed in idealized positions and were set riding on the respective parent atoms. All the non-H atoms were refined with anisotropic thermal parameters. Absence of additional symmetry and/or voids was confirmed by using PLATON. Olex2 was used for the thermal ellipsoidal plot (Fig. 1) [42-44].

RESULTS AND DISCUSSION

Formation of the Zn(II) complex. The scheme 1 represents the synthesis of the Zn(II) complex from the reaction of the indole thiosemicarbazone ligand with zinc(II) acetate in a methanol solution. The complex formation was confirmed by the elemental analysis and FT-IR, UV-Visible spectroscopic and single crystal X-ray diffraction studies. The complex was soluble in DMF and DMSO, partially soluble in $CHCl_3$ and CH_2Cl_2, and insoluble in other organic solvents.

Spectroscopy. The UV-Visible spectrum of the Zn(II) complex was recorded in DMF in the range 200-800 nm. The complex exhibited two bands at 260 nm and 322 nm, corresponding to $\pi \rightarrow \pi^*$ and $n \rightarrow \pi^*$ transitions respectively. A band at 395 nm due to the LMCT transition was also observed [45]. The peaks observed in the FT-IR spectrum of the Zn(II) complex at 3435 cm^{-1} and 3323 cm^{-1}, and 1509 cm^{-1} were assigned to ν(N–H) and ν(C=N) respectively. The C–S stretching frequency was noted at 721 cm^{-1}, which was not observed in the ligand.

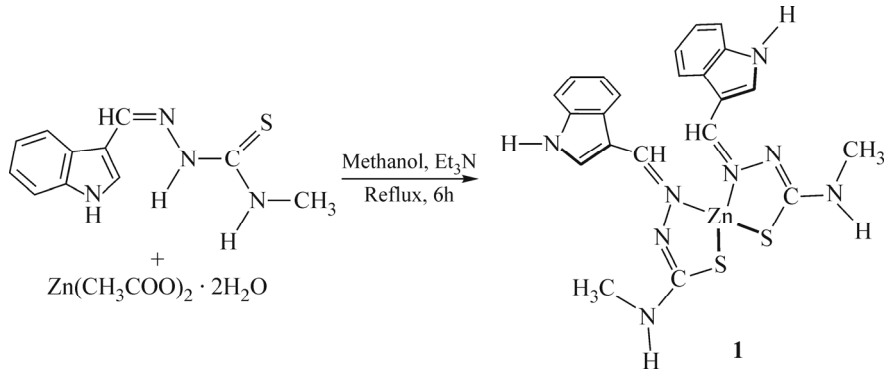

Scheme 1. Synthetic scheme for the Zn(II) complex bearing the indole thiosemicarbazone ligand.

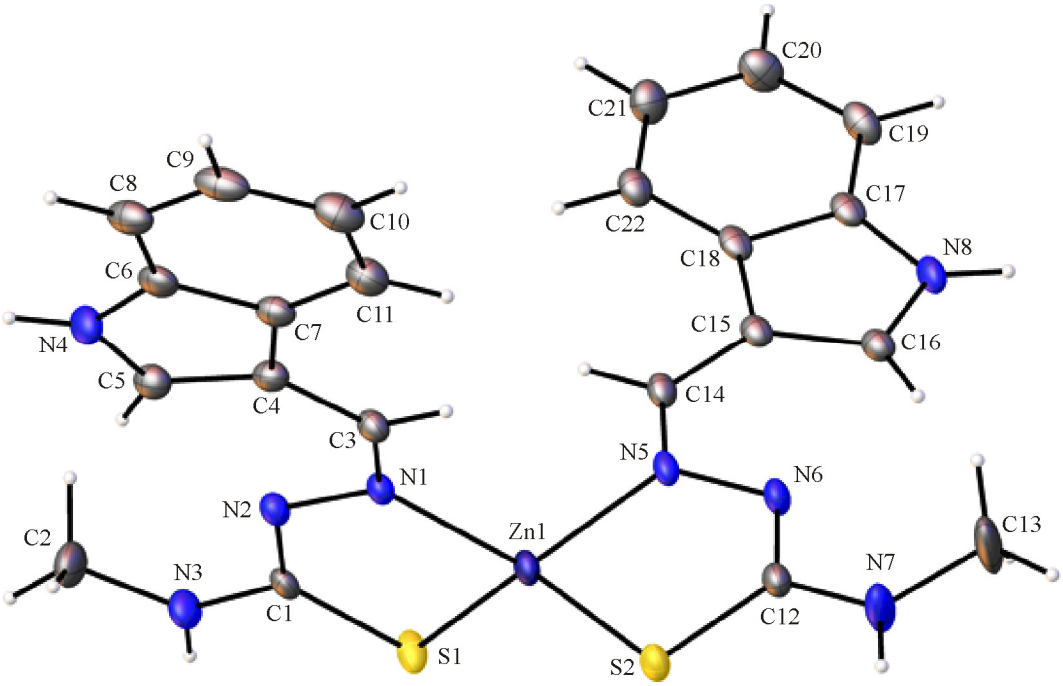

Fig. 1. The structure of solid complex **1** showing the atomic labelling scheme and thermal ellipsoids at the 50% probability level. Only one of the molecules in the asymmetric unit is shown for clarity. Space group: *P*-1 ($Z = 6$; $Z' = 3$). Selected bond distances (Å) and angles (deg): Zn(1)–S(1) 2.2593(7), Zn(1)–S(2) 2.2656(6), Zn(1)–N(1) 2.0169(19), Zn(1)–N(5) 2.0287(19), N(1)–Zn(1)–S(1) 87.93(6), N(5)–Zn(1)–S(2) 117.81(6), S(2)–Zn(1)–S(1) 126.72(3), N(5)–Zn(1)–N(1) 120.21(8).

Structure analysis. The structure of the Zn(II) complex is displayed in Fig. 1. The crystal data collection, structure solution, and refinement details are provided in Table 1. Selected bond distances, bond and torsion angles are given in Tables 2 and 3, respectively. The X-ray diffraction study confirmed the distorted tetrahedral structure of the Zn(II) complex which crystallized in the triclinic crystal system with the *P*-1 space group. Thiosemicarbazone coordinated to the Zn(II) ion as a monobasic bidentate [imine nitrogen (N-neutral) and thiocarbonyl sulfur (S-anionic)] ligand. The perfect tetrahedral/square planar geometry is reflected by the τ_4 parameter [46, 47] for a four-coordinated system. τ_4 can be calculated using the formula $\tau_4 = [360 - (\alpha + \beta)]/141°$, where α and β are the largest angles in the coordination sphere. The τ_4 value is 1.00, since $360 - 2(109.5) = 141$ for a perfect tetrahedral geometry, and is zero for a perfect square planar geometry since $360 - 2(180) = 0$. For an intermediate structure, e.g., trigonal pyramidal, τ_4 falls within the range 0-1.00. The distorted

TABLE 1. Crystallographic Data and Refinement Parameters

Parameter	**1**
Empirical formula	$C_{22}H_{22}N_8S_2Zn$
Formula weight	527.96
Temperature, K	100.0
Wavelength, Å	1.54178
Crystal system	Triclinic
Space group	*P*-1
Unit cell dimensions *a*, *b*, *c*, Å	9.1339(3), 21.0705(8), 21.1887(8)
α, β, γ, deg	118.4460(10), 90.345(2), 92.234(2)
Volume, Å^3; *Z*	3581.4(2); 6
Density (calculated), mg/m^3	1.469
Absorption coefficient, mm^{-1}	3.285
F(000)	1632
Crystal size, mm	0.276×0.222×0.126
θ range for data collection, deg	2.372 to 70.447
Index ranges	$-11 \le h \le 11$, $-25 \le k \le 22$, $0 \le l \le 25$
Reflections collected / independent; *R*(int)	13469 / 13469; 0.0878
Completeness to θ = 25.242°,%	99.1
Absorption correction	Semi-empirical from equivalents
Max. and min. transmission	0.753 and 0.525
Refinement method	Full-matrix least-squares on F^2
Data / restraints / parameters	13469 / 0 / 898
GOOF on F^2	1.045
Final *R* indices [$I > 2\sigma(I)$]	$R1 = 0.0369$, $wR2 = 0.0828$
R indices (all data)	$R1 = 0.0444$, $wR2 = 0.0862$
Largest diff. peak and hole, e/Å^3	0.784 and −0.533

TABLE 2. Selected Bond Lengths (Å) and Angles (deg)

Bond lengths	**1**	**1B**	**1D**
Zn(1/1B/1D)–S(1/1B/1D)	2.2593(7)	2.2808(6)	2.2572(7)
Zn(1/1B/1D)–S(2/2B/2D)	2.2802(6)	2.2751(7)	2.2677(6)
Zn(1/1B/1D)–N(1/1B/1D)	2.0169(19)	2.030(2)	2.016(2)
Zn(1/1B/1D)–N(5/5B/5B)	2.0287(19)	2.0123(19)	2.021(2)
Bond angles	**1**	**1B**	**1D**
S(2/2B/2D)–Zn(1/1B/1D)–S(1/1B/1D)	126.72(3)	129.47(3)	126.12(3)
N(1/1B/1D)–Zn(1/1B/1D)–S(1/1B/1D)	87.93(6)	86.73(6)	88.17(6)
N(1/1B/1D)–Zn(1/1B/1D)–S(2/2B/2D)	120.63(6)	116.26(6)	125.99(6)
N(5/5B/5D)–Zn(1/1B/1D)–S(1/1B/1D)	117.81(6)	121.83(6)	112.96(6)
N(5/5B/5D)–Zn(1/1B/1D)–S(2/2B/2C)	87.31(6)	88.10(6)	87.40(6)
N(5/5B/5D)–Zn(1/1B/1D)–N(1/1B/1D)	120.21(8)	117.65(8)	118.96(8)
C(1/1B/1D)–S(1/1B/1D)–Zn(1/1B/1D)	92.28(8)	92.59(8)	92.21(8)
C(12/12B/12D)–S(2/2B/2D)–Zn(1/1B/1D)	92.13(8)	91.99(8)	92.13(8)
N(2/2B/2D)–N(1/1B/1D)–Zn(1/1B/1D)	117.28(14)	118.64(15)	116.98(14)
C(3/3B/3D)–N(1/1B/1D)–Zn(1/1B/1D)	126.35(16)	123.72(16)	126.54(16)
N(6/6B/6D)–N(5/5B/5D)–Zn(1/1B/1D)	117.90(15)	116.81(14)	118.41(15)
C(14/14B/14D)–N(5/5B/5D)–Zn(1/1B/1D)	124.88(16)	127.61(16)	123.24(16)

TABLE 3. Selected Torsion Angles (deg)

Torsion angles	**1**	**1B**	**1D**
Zn(1/1B/1D)–S(1/1B/1D)–C(1/1B/1D)–N(2/2B/2D)	1.9(2)	2.6(2)	1.6(2)
Zn(1/1B/1D)–S(1/1B/1D)–C(1/1B/1D)–N(3/3B/3D)	–179.89(17)	–176.38(19)	–178.56(17)
Zn(1/1B/1D)–S(2/2B/2D)–C(12/12B/12D)–N(6/6B/6D)	1.0(2)	–1.8(2)	2.9(2)
Zn(1/1B/1D)–S(2/2B/2D)–C(12/12B/12D)–N(7/7B/7D)	179.9(2)	–179.32(18)	–177.90(19)
Zn(1/1B/1D)–N(1/1B/1D)–N(2/2B/2D)–C(1/1B/1D)	3.2(2)	–1.2(3)	3.5(2)
Zn(1/1B/1D)–N(1/1B/1D)–C(3/3B/3D)–C(4/4B/4D)	–174.37(19)	167.24(19)	–172.06(19)
Zn(1/1B/1D)–N(5/5B/5D)–N(6/6B/6D)–C(12/12B/12D)	–5.5(3)	–4.1(2)	–4.3(3)
Zn(1/1B/1D)–N(5/5B/5D)–C(14/14B/14D)–C(15/15B/15D)	–167.41(19)	176.03(18)	–169.7(2)

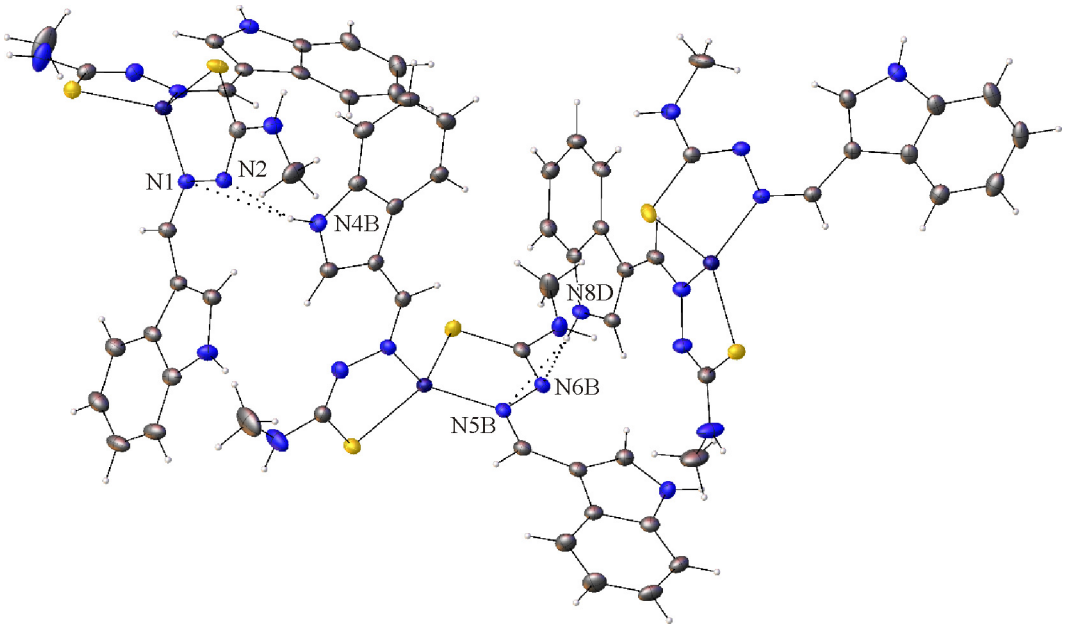

Fig. 2. Crystal packing view down the *a* axis exhibiting intermolecular interactions in complex **1**.

TABLE 4. Hydrogen Bonding Parameters (Å, deg)

D–H…A	*d*(D–H)	*d*(H…A)	*d*(D…A)	∠(DHA)
N(4)–H(4)…S(1B)$^{\#1}$	0.88	2.82	3.543(2)	139.8
N(7)–H(7)…S(2D)$^{\#2}$	0.88	2.53	3.410(2)	174.3
N(8)–H(8)…N(1D)$^{\#3}$	0.88	2.63	3.439(3)	154.2
N(8)–H(8)…N(2D)$^{\#3}$	0.88	2.19	3.060(3)	167.4
N(3B)–H(3B)…S(2)$^{\#4}$	0.88	2.65	3.518(2)	170.0
N(4B)–H(4B)…N(1)	0.88	2.17	3.021(3)	161.3
N(4B)–H(4B)…N(2)	0.88	2.78	3.429(2)	132.1
N(7B)–H(7B)…S(1D)$^{\#5}$	0.88	2.78	3.429(2)	132.1
N(8B)–H(8B)…S(2D)$^{\#5}$	0.88	2.74	3.493(2)	143.7
N(4D)–H(4D)…S(2)$^{\#6}$	0.88	2.71	3.512(2)	152.6
N(7D)–H(7D)…S(1B)$^{\#7}$	0.88	2.74	3.618(2)	171.5
N(8D)–H(8D)…N(5B)	0.88	2.47	3.314(3)	161.3
N(8D)–H(8D)…N(6B)	0.88	2.12	2.967(3)	162.0

Symmetry transformations used to generate equivalent atoms: $^{\#1}$ *x*–1, *y*, *z*; $^{\#2}$ *x*, *y*–1, *z*–1; $^{\#3}$ –*x*+1, –*y*+1, –*z*+1; $^{\#4}$ –*x*+1, –*y*, –*z*+1; $^{\#5}$ *x*+1, *y*, *z*; $^{\#6}$ –*x*, –*y*+1, –*z*+1; $^{\#7}$ –*x*+1, –*y*+1, –*z*+2.

tetrahedral geometry was found around Zn [S(2)–Zn(1)–S(1) 126.72(3), N(5)–Zn(1)–N(1) 120.21(8), N(5)–Zn(1)–S(1) 117.81(6), N(1)–Zn(1)–S(1) 87.93(6), N(1)–Zn(1)−S(2) 120.63(6), and N(5)–Zn(1)–S(2) 87.31(6)]. The τ_4 value for the Zn(II) complex was calculated as 0.798, which was near to 1, suggesting a distorted tetrahedral geometry around Zn(II) [6]. There was an increase in the C–S and C–N bond distances and a decrease in the N(1)–N(2) bond distance in the Zn(II) complex, as compared to the corresponding ligand [36-38]. The crystal packing was stabilized by intermolecular interactions (Fig. 2). The intermolecular hydrogen bonding parameters are listed in Table 4.

CONCLUSIONS

In summary, zinc(II) complex $[Zn(C_{11}H_{11}N_4S)_2]$ (**1**) was synthesized from the indole thiosemicarbazone ligand and zinc(II) acetate. The new complex was characterized by the elemental analysis and spectroscopic studies. The molecular structure of $[Zn(C_{11}H_{11}N_4S)_2]$ (**1**) was solved by the single crystal X-ray diffraction method. The complex exhibited a distorted tetrahedral geometry around the Zn(II) ion. The crystal packing diagram and hydrogen bonding interactions showed the supramolecular nature of the complex.

ADDITIONAL INFORMATION

CCDC 1907485 contains the supplementary crystallographic data for **1**. These data can be downloaded free of charge form the Cambridge Crystallographic Data Center *via* www.ccdc.cam.ac.uk/datarequest.cif or from the Cambridge Crystallographic Data Centre (CCDC), 12 Union Road, Cambridge CB2 1EZ, UK; fax: +44(0)1223-336033 or e-mail: deposit@ccdc.cam.ac.uk.

CONFLICT OF INTERESTS

The authors declare that they have no conflict of interests.

REFERENCES

1. I. E. Dreosti. *Mutat*. *Res*., **2001**, *475*, 161–167.
2. A. S. Prasad. *J*. *Am*. *Coll*. *Nutr*., **1998**, *17*, 542–543.
3. A. S. Prasad and O. Kucuk. *Cancer Metastasis Rev*., **2002**, *21*, 291–295.
4. A. S. Prasad. *Br*. *Med*. *J*., **2003**, *326*, 409–410.
5. T. M. Bray and W. J. Bettger. *Free Radic*. *Biol*. *Med*., **1990**, *8*, 281–291.
6. S. R. Powell. *J*. *Nutr*., **2000**, *130*, 1447S–154S.
7. A. Tarushi, P. Kastanias, C. P. Raptopoulou, V. Psycharis, D. P. Kessissoglou, A. N. Papadopoulos, and G. Psomas. *J*. *Inorg*. *Biochem*., **2016**, *163*, 332–345.
8. C. P. Larson, U. R. Saha, and H. Nazrul. *PLoS Med*., **2009**, *6*, e1000175.
9. E. C. Fusch and B. Lippert. *J*. *Am*. *Chem*. *Soc*., **1994**, *116*, 7204–7209.
10. J. d′Angelo, G. Morgant, N. E. Ghermani, D. Desmaele, B. Fraisse, F. Bonhomme, E. Dichi, M. Sghaier, Y. Li, Y. Journaux, and J. R. J. Sorenson. *Polyhedron*, **2008**, *27*, 537–546.
11. H. Sakurai, Y. Kojima, Y. Yoshikawa, K. Kawabe, and H. Yasui. *Coord*. *Chem*. *Rev*., 2**002**, *226*, 187–198.
12. Q. Zhou, T. W. Hambley, B. J. Kennedy, P. A. Lay, P. Turner, B. Warwick, J. R. Biffin, and H. L. Regtop. *Inorg*. *Chem*., **2000**, *39*, 3742–3748.
13. N. C. Kasuga, K. Sekino, M. Ishikawa, A. Honda, M. Yokoyama, S. Nakano, N. Shimada, C. Koumo, and K. Nomiya. *J*. *Inorg*. *Biochem*., **2003**, *96*, 298–310.
14. Z. Li, F. Wu, Y. Gong, C. Hu, Y. Zhang, and M. Gan. *Chin*. *J*. *Chem*., **2007**, *25*, 1809–1814.

15. Z. Chen, R. Xiong, J. Zhang, X. Chen, Z. Xue, and X. You. *Inorg. Chem.*, **2001**, *40*, 4075–4077.
16. M. P. Lopez-Gresa, R. Ortiz, L. Perello, J. Latorre, M. Liu-Gonzalez, S. Garcia-Granda, M. Perez-Priede, and E. Canton. *J. Inorg. Biochem.*, **2002**, *92*, 65–74.
17. D. Xiao, E. Wang, H. An, Z. Su, Y. Li, L. Gao, C. Sun, and L. Xu. *Chem. Eur. J.*, **2005**, *11*, 6673–6686.
18. A. Tarushi, K. Lafazanis, J. Klun, I. Turel, A.A. Pantazaki, G. Psomas, and D. P. Kessissoglou. *J. Inorg. Biochem.*, **2013**, *121*, 53–65.
19. A. Tarushi, Z. Karaflou, J. Kljun, I. Turel, G. Psomas, A. N. Papadopoulos, and D. P. Kessissoglou. *J. Inorg. Biochem.*, **2013**, *128*, 85–96.
20. A. Tarushi, X. Totta, A. Papadopoulos, J. Kljun, I. Turel, D. P. Kessissoglou, and G. Psomas. *Eur. J. Med. Chem.*, **2014**, *74*, 187–198.
21. J. S. Casas, E. E. Castellano, M. D. Couce, J. Ellena, A. Sanchez, J. Sordo, and C. Taboada. *J. Inorg. Biochem.*, **2006**, *100*, 124–132.
22. Z. Travnicek, V. Krystof, and M. Sipl. *J. Inorg. Biochem.*, **2006**, *100*, 214–225.
23. M. Di Vaira, C. Bazzicalupi, P. Orioli, L. Messori, B. Bruni, and P. Zatta. *Inorg. Chem.*, **2004**, *43*, 3795–3797.
24. A. K. McCall, H. Chih-chin, and C. A. Fierke. *J. Nutr.*, **2000**, *130*, 1437S–1446S.
25. J. Osredkar and N. Sustar. *J. Clinic Toxicol.* **2011**, *S3*, 1–18.
26. R. Donovick, F. Pansy, G. Stryker, and J. Bernstein. *J. Bacteriol.*, **1950**, *59*, 667–674.
27. G. Domagk, R. Behnisch, F. Mietzsch, and H. Schmidt. *Naturwissenschaften*, **1946**, *33*, 315.
28. A. E. Liberta and D. X. West. *Biometals*, **1992**, *5*, 121–126.
29. D. L. Klayman, J. F. Bartosevich, T. S. Griffin, C. J. Mason, and J. P. Scovill. *J. Med. Chem.*, **1979**, *22*, 855–862.
30. D. Hamre, J. Bernstein, and R. Donovick. *Proc. Soc. Exp. Bio. Med.*, **1950**, *73*, 275–278.
31. C. Shipman Jr., S. H. Smith, J. C. Drach, and D. L. Klayman. *Antiviral Res.*, **1986**, *6*, 197–222.
32. K. A. Brownlee and D. Hamre. *J. Bacteriol.*, **1951**, *61*, 127–134.
33. R. W. Brockman, J. R. Thomson, M. J. Bell, and H. E. Skipper. *Cancer Res.* **1956**, *16*, 167–170.
34. T. S. Lobana, R. Sharma, G. Bawa, and S. Khanna. *Coord. Chem. Rev.*, **2009**, *253*, 977–1055.
35. A. A. Ibrahim, H. Khaledi, P. Hassandarvish, H. M. Ali, and H. Karimian. *Dalton Trans.*, **2014**, *43*, 3850–3860.
36. J. Haribabu, K. Jeyalakshmi, Y. Arun, N. S. P. Bhuvanesh, P. T. Perumal, and R. Karvembu. *J. Biol. Inorg. Chem.*, **2017**, *22*, 461–480.
37. J. Haribabu, G. Sabapathi, M. Muthu Tamizh, C. Balachandran, N. S. P. Bhuvanesh, P. Venuvanalingam, and R. Karvembu. *Organometallics*, **2018**, *37*, 1242–1257.
38. J. Haribabu, M. Muthu Tamizh, C. Balachandran, Y. Arun, N. S. P. Bhuvanesh, A. Endo, and R. Karvembu. *New J. Chem.*, **2018**, *42*, 10818–10832.
39. APEX3 "Program for Data Collection on Area Detectors" BRUKER AXS Inc., 5465 East Cheryl Parkway, Madison, WI 53711-5373 USA.
40. G. M. Sheldrick. TWINABS. "Program for Absorption Correction of Area Detector Frames", BRUKER AXS Inc., 5465 East Cheryl Parkway, Madison, WI 53711–5373 USA.
41. G. M. Sheldrick. *Acta Crystallogr.*, **2008**, *A64*, 112–122.
42. G. M. Sheldrick. *Acta Crystallogr.*, **2015**, *A71*, 3–8.
43. G. M Sheldrick. *Acta Crystallogr.*, **2015**, *C71*, 3–8.
44. O. V. Dolomanov, L. J. Bourhis, R. J. Gildea, J. A. K. Howard, and H. Puschmann. *J. Appl. Cryst.*, **2009**, *42*, 339–341.
45. K. N. Anees Rahman, J. Haribabu, C. Balachandran, N. S. P. Bhuvanesh, R. Karvembu, and A. Sreekanth. *Polyhedron*, **2017**, *135*, 26–35.
46. P. Murrayrust, H. B. Burgi, and J. D. Dunitz. *J. Am. Chem. Soc.*, **1975**, *97*, 921–922.
47. S. Keinan and D. Avnir. *J. Chem. Soc. Dalton Trans.*, **2001**, *6*, 941–947.